DISLOCATION STRUCTURE AND LOW FREQUENCY MECHANICAL HYSTERESIS IN COPPER SINGLE CRYSTALS†

J. Dralla and J. C. Bilello
Department of Materials Science
State University of New York at Stony Brook
Stony Brook, New York 11790

ABSTRACT

Copper single crystals of several orientations were grown and sectioned at various stages of prestrain such that both primary and forest dislocations could be directly observed using etch-pit techniques. Half-cycle hysteresis loops, at positive stress bias, representing damping frequencies in the range of $\approx 10^{-1}$ Hz were performed on these samples at room temperature. The results of the etch-pit and mechanical damping studies were correlated, and a model was formulated which describes the damping in terms of a dislocation-dislocation interaction model. The controlling pinning mechanism was associated with primary forest dislocation combinations, and a discussion of the appropriate binding energy is made.

† This work was supported in part by the U. S. Atomic Energy Commission.

DISLOCATION STRUCTURE AND LOW FREQUENCY MECHANICAL HYSTERESIS IN COPPER CRYSTALS

INTRODUCTION

Amplitude-dependent internal friction in metals, at high frequencies, is generally thought to be hysteretic and associated with the interaction of the entire Frank network of dislocations with discrete impurity atoms in the lattice (1,2,3,4). The dislocation unpins from the impurity atom by a combination of stress and thermal activation with typical binding energies of the order of 0.1eV (5,6). Low frequency mechanical damping has been observed in the $\approx 10^{-1}$ Hz range and it was originally suggested that both types of damping were of similar origin (7). However, recent evidence has cast considerable doubt on this earlier interpretation (8,9) and instead has postulated that the latter range of damping is caused by primary dislocation-forest dislocation interactions with binding energies ~1eV. If the forest pinning model governs, then a unique opportunity presents itself to make a direct correlation between a particular range of damping behavior and the pinning mechanism responsible for the hysteresis. The present experiments report the results of comparing the forest and primary dislocation structures observed

from etch-pit analysis with the low frequency damping behavior of copper crystals of several orientations.

EXPERIMENTAL PROCEDURE

A modified Bridgman technique was used to grow copper crystals in vacuum from 99.999% grade material purchased from ASARCO. The crystals were acid-sawed into samples which had 25mm gage lengths and square cross-sectional areas of 22.5 mm^2. The tensile axes of the orientations studied are shown in Fig. 1 with: crystal A 19° from (100), B 14° from (110), and C 2° from (112); because of the proximity to these directions crystals A, B, C will be designated by these indices in the remainder of the text. These crystals were chosen at these orientations to represent the general range of slip character that can occur for f.c.c. copper. All crystals were annealed in vacuum for 24 hours, in graphite trays, at 1070°C and then furnace cooled. Samples were chosen after this anneal so that for all orientations the initial grown-in density of dislocations was 2×10^6 cm^{-2}, with an average sub-boundary spacing of ~½ mm.

Tensile tests were performed on an Instron machine using a strain rate 1.7×10^{-4} $sec.^{-1}$ for prestraining and of 10^{-6} $sec.^{-1}$ for performing the low frequency damping experiments. A high strain resolution microstrain network capable of displacement sensitivities of ~1×10^{-7} in. was employed in these experiments. A detailed description of

the microstrain apparatus and calibration procedure for drift, linearity, and sensitivity appears elsewhere (8,10).

A one micron crack-free chromium film was plated on all samples, because it was found convenient to extend the amplitude range of the decrement at any particular prestrain. The influence of the film and a discussion of any possible surface effect related to low frequency mechanical hysteresis have already been treated (8,11).

It was important to be able to observe both the primary and forest-dislocation densities for each crystal in order to independently determine the number of primary dislocation loops and the number of possible forest pins available. In order to accomplish this, crystals were sectioned and polished along the appropriate {111} planes using a procedure similar to YOUNG and WILSON (1961)(12), and then these surfaces were etched to reveal the dislocation structure using LIVINGSTON (1960)(13).

RESULTS AND DISCUSSION

General

In studying the influence of structure on low frequency mechanical damping behavior, the amplitude dependence of the decrement was taken at prestrains chosen so that the three orientations which were studied had a large range of overlap (e.g. samples at (110) orientation with prestrains ≈ 0.025 showed damping only over a 150gm/mm^2 to 300gm/mm^2). Also, it was necessary to keep the amount

of prior deformation small enough so that the dislocation densities could be determined by etch-pit methods; yet large enough so that a significant range of amplitude dependence could be observed. Table I, column 1 reports the results of the primary densities measured for the three crystals. The second aim was to keep the forest densities approximately constant (column 2, Table I) and this was accomplished by experimentation using as a guideline the stress-forest density relationship of BASINSKI and BASINSKI (14). Thus it was possible to vary the number of primary loops by about a factor of 2 while the number of available forest junctions stayed approximately constant. The amplitude dependence of the decrement is shown in Fig. 2 for the crystals reported in Table I. Virtually no amplitude dependence is associated with (112) and even for the other two cases the dependence is rather small compared with that observed in the KHz range.

TABLE I

Measured etch-pit values

Crystal	ρ_p Primary density (cm^{-2})	ρ_f Forest density (cm^{-2})	$\bar{\ell}_f$ (cm)	Prestress (gm/cm^2)
(110)	3.5×10^7	9.6×10^6	3.2×10^{-4}	774
(100)	6.0×10^7	1.1×10^7	3.0×10^{-4}	550
(112)	8.0×10^7	1.3×10^7	2.8×10^{-4}	595

Fig. 3 illustrates the orientation dependence of the decrement, Δ, over the amplitude range where the data in Fig. 2 coincides. The amplitude dependence is seen to be largest for the (110) crystal and becomes smaller as the stress axis moves from (100) through (112) directions. This effect is analogous to the prestrain dependence of the decrement at fixed orientation, which is shown in Fig. 4. In the strain-dependent case, the primary density for f.c.c. copper increases through work-hardening Stage I, but the forest density remains essentially unchanged (14). The conclusion, that is suggested by the results shown in Figs. 3 and 4, is that the amplitude dependence of the decrement for low frequency damping is independent of the mode in which a particular dislocation structure is produced, (i.e. either by producing relatively constant prestrains at various orientations or by varying the amount of prestrain for a fixed orientation).

DISLOCATION STRUCTURE

In the present experiments, both the primary and forest dislocation structures were measured directly using the method described in the experimental procedure section. A photo-micrograph of a typical forest plane section before and after prestrain is shown in Fig. 5. The section obtained before straining was produced from a section of the crystal immediately adjacent to the gage length at either end of the sample. About an order of magnitude rise in the forest density is apparent even though the sample was still in work-hardening Stage I. This is generally the case for

coated crystals since secondary slip occurs before a well developed Stage II hardening is observed in the macroscopic stress-strain curve. The observed increase in forest density agrees with the stress-forest density relationship of others (14). The complete etch-pit data for all crystals appears in Table I.

Previous work on low frequency mechanical hysteresis has not correlated directly measured damping behavior with structures. The dislocation structures have either been inferred from the dislocation measurements of others (8) or have been calculated from the assumed damping model (15). In the next section a simplified damping model will be chosen and the magnitude of the damping level calculated from the measured etch-pit arrays.

Mechanism for Energy Loss

It has been shown earlier (8,15) that the modulus defect can be quite large, of the order of 15-25% for low frequency hysteresis experiments. This defect was found to be almost entirely caused by the large bowing strains associated with the excess primary loops produced by the plastic deformation (8). Furthermore, at the large stress amplitudes which have been used here, i.e. up to $\simeq \frac{1}{2}$ the flow stress, all loops have already broken away from impurity pins at stress levels equivalent to the preload level in the present experiments (8).

The strongest primary-forest dislocation interaction is assumed to be that between attractive triple point junctions (16). Fig. 6 shows a sequence which illustrates

the motion of a primary loop pinned at three triple nodes (T). As the stress is increased, the loop breaks away from the weaker nodes; longer loops will generally break away first, if all nodes are of approximately the same binding energy. On reversing the stress, the loops collapse back and recombine. The general physical feature of the dislocation-strain vs. stress is analogous to that originally envisioned for impurity pinning in the GRANATO-LÜCKE model (4). Yet for all the similarities, there are still some very important differences. These are: 1) binding energy of pinning agent is about an order of magnitude higher than for impurities, 2) there are no fixed node points since the nodes can move under the applied stress, and 3) bowing strain is very large, of the order of 10^{-4}, and hence the assumption of small dislocation curvatures becomes untenable.

At low stress amplitudes, when the first loops break away, the dislocation array is similar to a collection of double loops. For this case, a quantitative comparison of the decrement level with dislocation structure can be made.

The decrement is given by $\Delta \approx 2\delta a/a$ where δa is the dislocation strain and a is the elastic shear strain (16). For f.c.c. copper, more than one slip system is operative, so that for the i^{th} system:

$$a_i = \frac{N_i \ell_i^3 \tau_i}{6\mu} \qquad (1)$$

Where, N_i are the number of loops, ℓ_i the loop length, τ_i the resolved shear stress all for the i^{th} slip system. The appropriate shear modulus is μ.

The decrement is then given by $\Delta \approx 2\delta\mu/\mu \approx 2\delta a/a$ so that from Equation (2):

$$\Delta \approx \sum_i \left(\frac{A_i N_i \ell_i^3}{3} \right) \qquad (2)$$

summed over all twelve slip systems. A_i is a distribution factor proportional to the stress operating on each slip system. If the number of dislocations on the primary is equal to that on another slip system, i.e. $\rho_p \approx \rho_f$ and the systems are equally stressed, then a significant proportion of the decrement would be due to dislocations lying on slip systems other than the primary. This could presumably be the case only at large strains in Stage II for all crystal orientations studied in the present experiments. The (112) crystal would also be subject to this full summation at small strains; since both the primary and conjugate slip systems are nearly equally stressed, $\tau_c/\tau_p = 0.93$, but at the prestrain used here $\rho_p >> \rho_f$ so that only a few percent correction is introduced considering terms in the summation other than that due to the primary system. Thus for all crystals in the prestrain range considered $A_i \approx \begin{cases} 1, & i = 1 \\ 0, & 2 \leq i \leq 12 \end{cases}$

Fig. 6 illustrates the basis of applying Equation (2) to the dislocation-dislocation interaction model. The distance between attractive junctions is a factor α times the forest spacing. For a random three

dimensional network $\alpha = 3$, but for prestrained crystals, with forest multiplication, α is more nearly equal to 2(16). The loop length for the expanded double loop can then be seen to be $\simeq 4\bar{\ell}_f$, where $\bar{\ell}_f$ is the modal forest spacing* taken from $\rho_f^{-\frac{1}{2}} \approx \bar{\ell}_f$. The number of primary loops is likewise obtained from the measured values in Table I, i.e. $2\rho_p \approx N_p$ (cm^{-3}). The decrement is thus from Eqn(2):

$$\Delta \cong \frac{N_p(4\bar{\ell}_f)^3}{3} \qquad (3)$$

The initial values of the decrement for the three crystals, calculated from Eqn(3) using the data in Table I, are:

Δ (110) = 0.013, Δ (100) = 0.018, Δ (112) = 0.018.

These are in good agreement with the initial decrements observed in Fig. 2 for the three crystals.

The amplitude-dependence, on the basis of this model, can arise from; 1) the activation of shorter loops with increasing applied stress, 2) breakdown of stronger junctions, 3) dislocations which have already broken-away becoming multi-loops i.e. a progressive breakdown of the primary dislocation - forest dislocation combinations. This view is consistent with etch-pit studies of the processes leading to yielding in copper crystals. (17,18).

Some final comments should be made concerning the binding energy associated with primary-forest dislocation combinations. The amplitude-dependent damping caused by impurity-dislocation interactions, which has been discussed by Granato-Lücke, leads to binding energies of the order of

---

* Because Δ is a very sensitive function of $\bar{\ell}_f$; careful statistics were taken for ρ_f. At least 2×10^4 etch-pits were counted for ρ_f on each crystal, with 90% of the $\bar{\ell}_f$ values falling within ±20% of the modal values for the prestrains used here.

o.leV (4). The process considered here is formally the same, i.e. hysteretic, with the forest-primary attractive junctions forming the "weak pins" and the incipient cell structure the strong nodes which limit catastrophic breakaway. The structures shown in Fig. 5 indicate that the forest is not homogeneous and that as a first approximation this idealized view is in reasonable qualitative agreement with the observed forest dislocation arrangements. This model can be checked for plausibility by calculating the binding energy which would be associated with the data reported in Table I. From TEUTONICO, GRANATO, and LÜCKE (6) the binding energy U_o required for mechanical breakaway is given by:

$$U_o \approx \sigma_o b^2 \ell \qquad (4)$$

where σ_o is the breakaway stress, taken here as the value of the minimum shear stress amplitude at which damping is observed. Thus, from Fig. 2 $\sigma_o \approx 100 g/mm^2$; b is the burgers vector, 2.5×10^{-8}cm; and ℓ is the spacing between pinning points, which is $\approx 3 \times 10^{-4}$cm from Table I. Using these results, one finds that $U_o \approx$ leV which is in line with the values expected from the assumed forest-primary dislocation model.

The correlation between dislocation structure and low frequency mechanical hysteresis, given here, provides reasonable evidence that primary dislocation - forest dislocation interactions control the damping behavior in this low frequency, high amplitude range.

ACKNOWLEDGEMENTS

The authors wish to thank Mr. J. Pridans for his help in the etch-pit measurements and Mr. K. Tandon for building the acid-sectioning device.

REFERENCES

1. T.A. READ, Trans. AIME, 143,30, (1941).

2. A.S. NOWICK, Phys. Rev., 80, 249, (1950).

3. J. WEERTMAN and E.I. SALKOVITZ, Acta Met., 3, 1, (1955).

4. A.V. GRANATO and K. LÜCKE, J.Appl. Phys., 27, 583, 789, (1956).

5. J. FRIEDEL, N.P.L. No.15, The Relation between the Structure and Mechanical Properties of Metals, p.409, (1963).

6. L.J. TEUTONICO, A.V. GRANATO, and K. LÜCKE, J. Appl.Phys., 35, 220, (1964).

7. J.M. ROBERTS, and N. BROWN, Trans. AIME, 218, 454, (1960)

8. J.C. BILELLO and M. METZGER, J. Appl. Phys., 38, 849, (1967).

9. J.M. ROBERTS, PROCEEDING I.C.S.M.A., Suppl. Trans., J.I.M., 9, 69, (1968).

10. J.C. BILELLO, Phil. Mag., 19, 583, (1969).

11. J.C. BILELLO and M. METZGER, Scripta Met., 2, 581, (1968).

12. F.W. YOUNG, JR. and T.R. WILSON, Rev. Sci. Inst., 32, 559, (1961).

13. J.D. LIVINGSTON, J. Appl. Phys., 31, 1071 (1960).

14. Z.S. BASINSKI and S.J. BASINSKI, Phil. Mag., 9, 51 (1964).

15. J.M. ROBERTS and N. BROWN, Acta Met., 10, 430 (1962).

16. J. FREIDEL, DISLOCATIONS (Addison-Wesley, Reading, Mass.) p.222, 357, (1964).

17. F.W. YOUNG, JR., J. Appl. Phys., 32, 1815, (1961).

18. A.S. ARGON, and W.T. BRYDGES., Phil, Mag., 18, 817, (1968).

FIGURE CAPTIONS

Fig. 1 Orientation of longitudinal axis for the three crystals.

Fig. 2 Amplitude-dependence of the decrement, Δ, at the indicated prestrains a_p for each orientation. Stress, σ, is the axial conponent.

Fig. 3 Orientation dependence of the decrement for the three crystals with common forest dislocation densities i.e. nearly constant density and distribution of nodes. Stress-amplitude indicated on each curve is in (g/mm^2).

Fig. 4 Prestrain dependence of the decrement at constant orientation, for an easy glide crystal, longitudinal axis 8° from (110). Stress-amplitude indicated on each curve is in (g/mm^2). (plot obtained from data in Ref. 8).

Fig. 5 Microphotographs of the forest dislocation structure for crystal A (100). Upper photo taken before straining and lower after a prestrain of ≈ 0.025. About an order of magnitude increase in dislocation density occurred. Magnifications indicated on photos.

Fig. 6 Schematic illustrating mode in which mechanical hysteresis can arise from primary-forest dislocation interaction. Solid lines represent a primary dislocation which lies on the slip plane (plane of page). Dotted lines are the forest dislocations which thread through the slip plane. Where the primary and forest dislocations intersect a short segment of recombination occurs and a pair of triple nodes is formed, indicated by a T. Under stress primary bows out (1) junctions break down with increasing stress, (2),(3),(4). On relaxing the stress, primary dislocation moves back and the nodes (T) are reformed.

Fig. 1
J.D. + J.C.B.

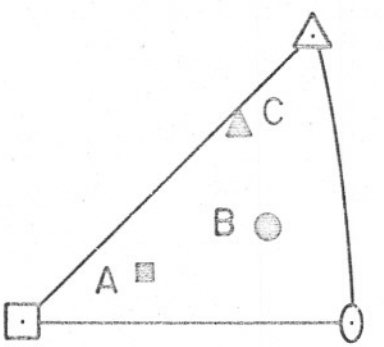

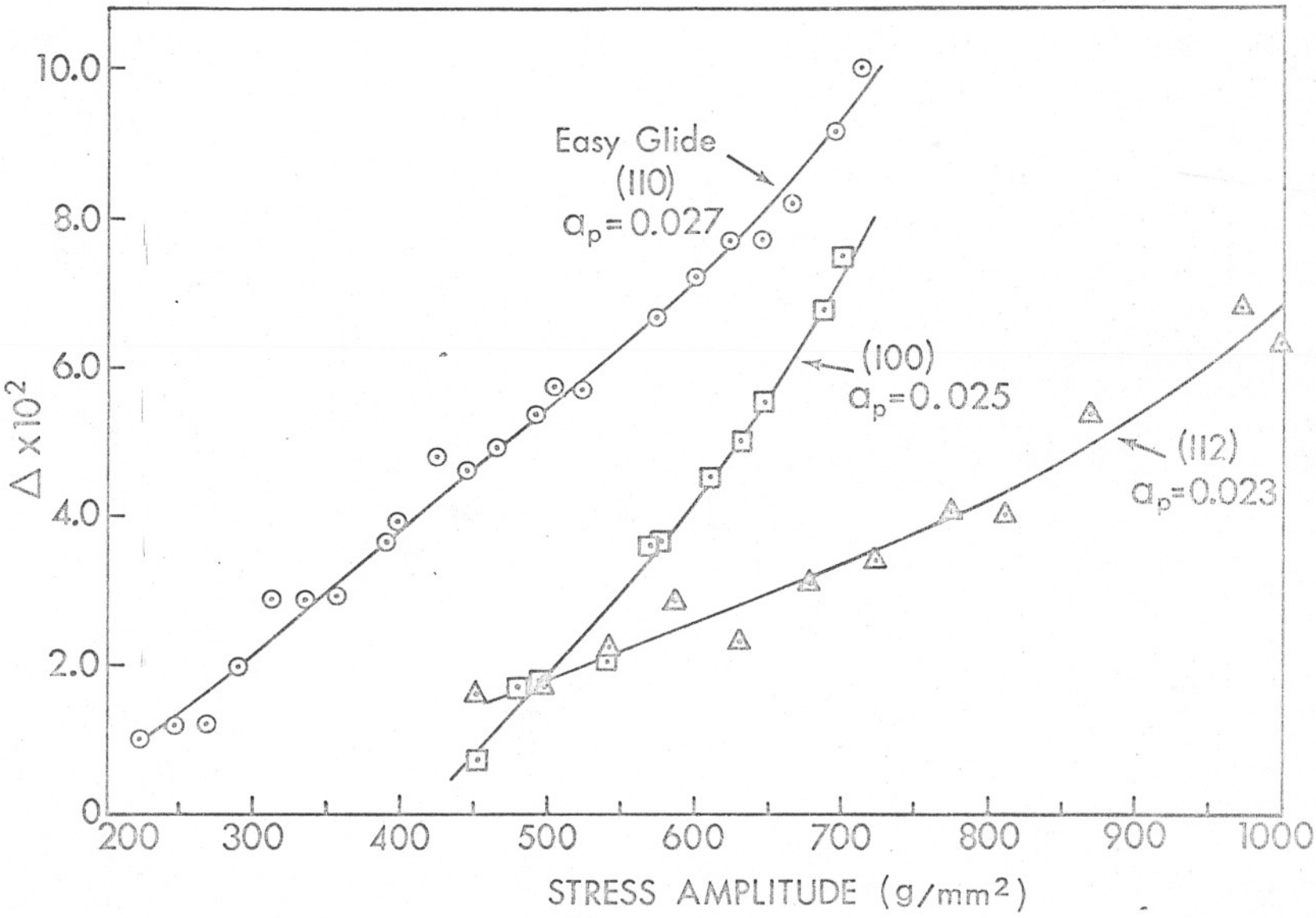
10.0
8.0
6.0
4.0
2.0
0
Δ x10²
200
300
400
500
600
700
800
900
1000
STRESS AMPLITUDE (g/mm²)
Easy Glide
(110)
a_p = 0.027
(100)
a_p = 0.025
(112)
a_p = 0.023

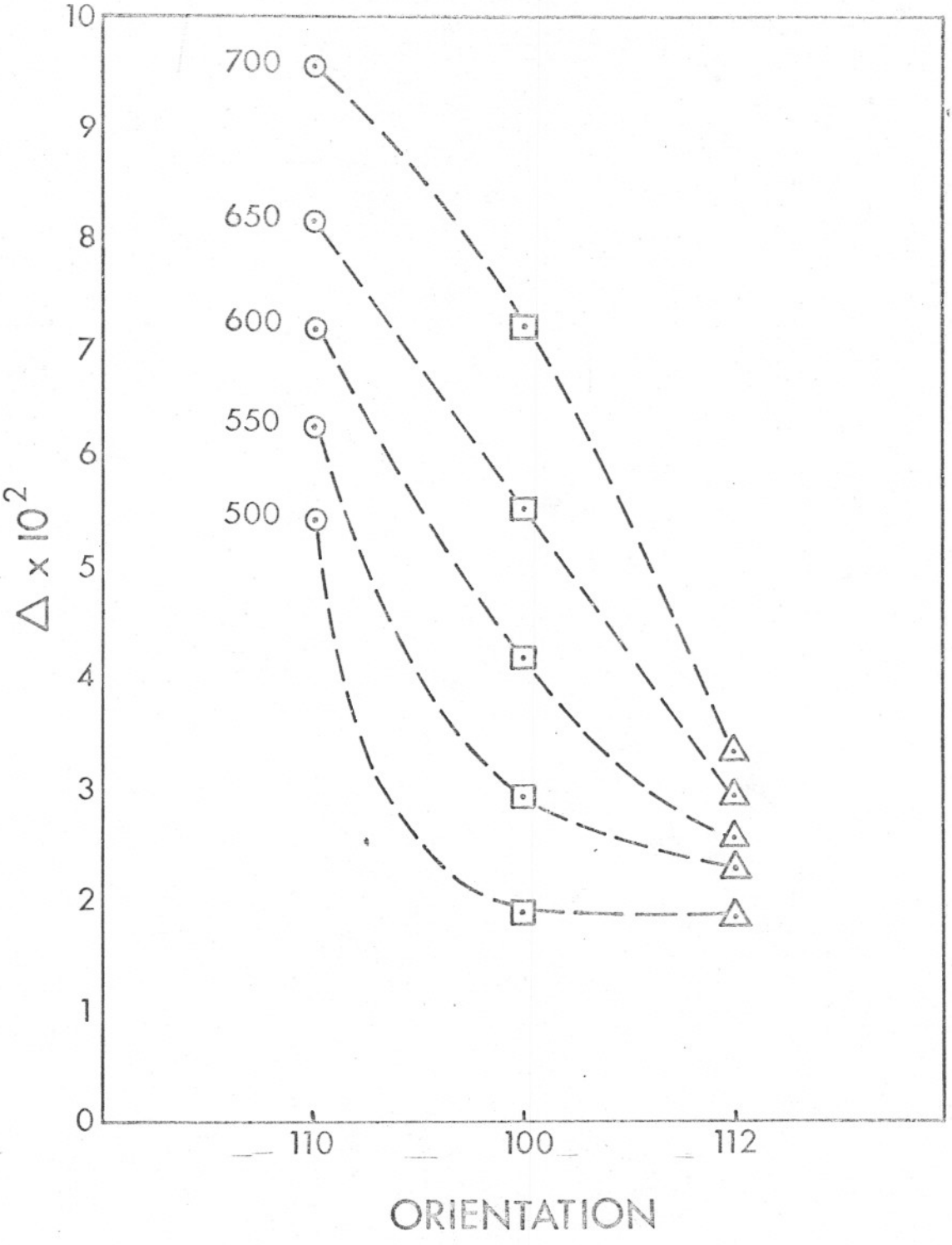
10
9
8
7
6
5
4
3
2
1
0
700
650
600
550
500
Δ x 10²
110
100
112
ORIENTATION

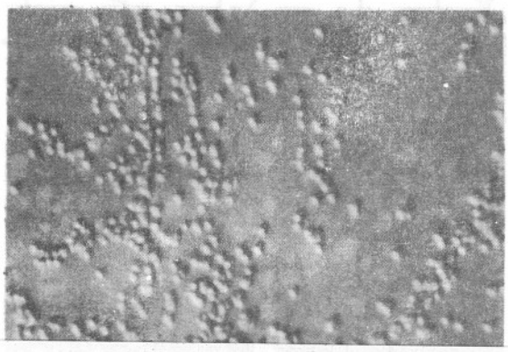

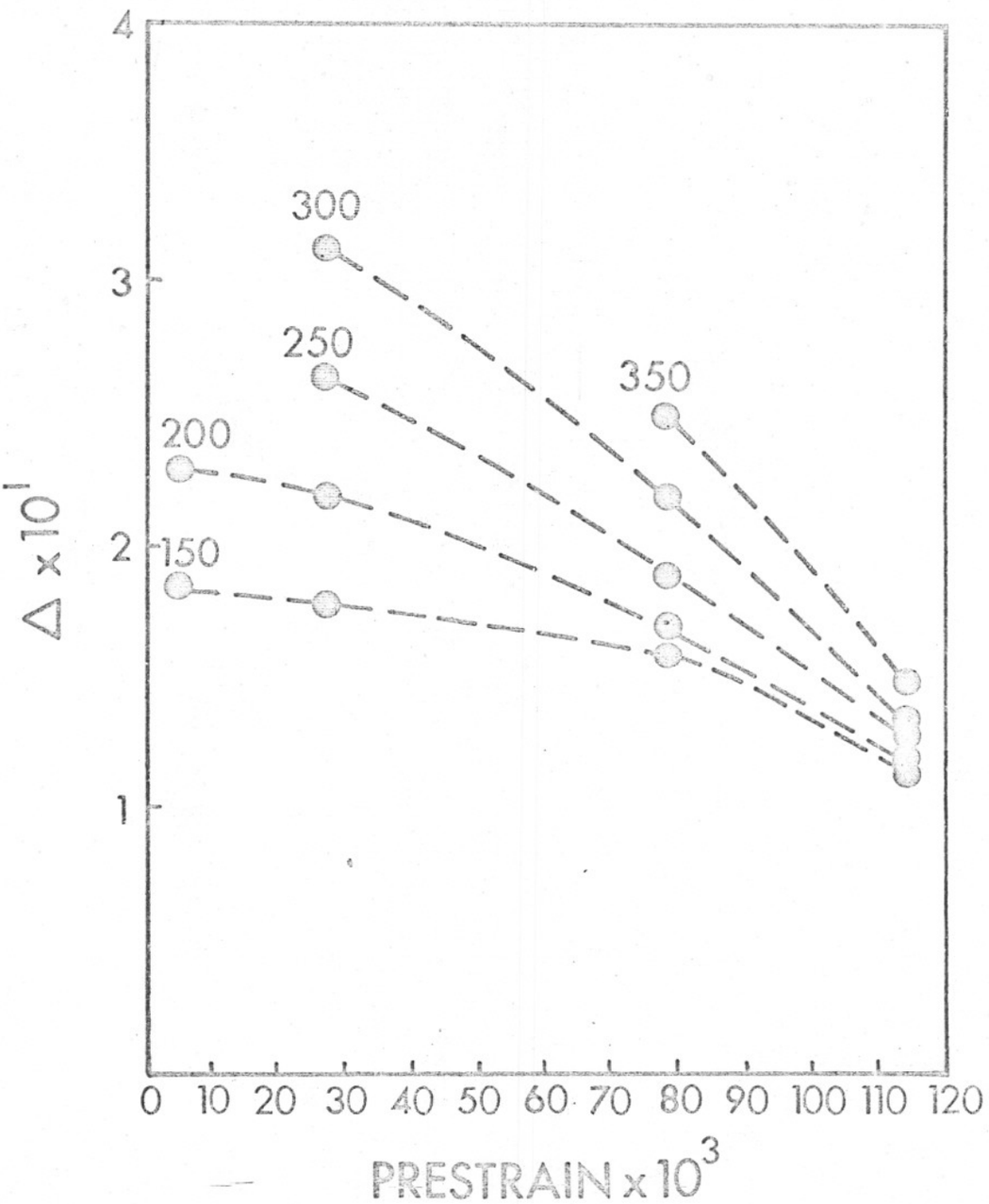
4
3
2
1
300
250
200
150
350
Δ x 10⁻¹
0 10 20 30 40 50 60 70 80 90 100 110 120
PRESTRAIN x 10³